Published in final edited form as:
Cancer Res. 2012 July 1; 72(13): 3135–3142. doi:10.1158/0008-5472.CAN-11-3195.

Stat3 Activation in Urothelial Stem Cells Leads to Direct Progression to Invasive Bladder Cancer

Philip Levy Ho[1], **Erica Julianne Lay**[1,2], **Weiguo Jian**[1], **Diana Parra**[1], and **Keith Syson Chan**[1,2,3]

[1]Department of Urology, Baylor College of Medicine, Houston, Texas

[2]Department of Molecular & Cellular Biology, Baylor College of Medicine, Houston, Texas

[3]Dan L Duncan Cancer Center, and Center for Cell Gene and Therapy, Baylor College of Medicine, Houston, Texas

Abstract

Two subtypes of human bladder cancer, noninvasive papillary and muscle-invasive cancer, develop through independent pathologic and molecular pathways. Human invasive bladder cancer frequently develops without prior clinical evidence of a noninvasive tumor stage. However, an animal model that recapitulates this unique clinical progression of invasive bladder cancer has not yet been developed. In this study, we created a novel transgenic mouse model of invasive bladder cancer by targeting an active dimerized form of Stat3 to the basal cells of bladder epithelium. When exposed to the carcinogen nitrosamine, Stat3-transgenic mice developed invasive cancer directly from carcinoma *in situ* (CIS), bypassing the noninvasive papillary tumor stage. Remarkably, invasive bladder cancer driven by active Stat3 was predominantly composed of stem cells, which were characterized by cytokeratin 14 (CK14) staining and enhanced tumor sphere-forming ability. Active Stat3 was also shown to localize to the nucleus of human invasive bladder cancers that were primarily composed of $CK14^+$ stem cells. Together, our findings show that Stat3-induced stem cell expansion plays a critical role in the unique clinical progression of invasive bladder cancer through the CIS pathway.

Corresponding Author: Keith Syson Chan, Departments of Urology and Molecular & Cellular Biology, Dan L Duncan Cancer Center, and Center for Cell Gene and Therapy, Baylor College of Medicine, One Baylor Plaza BCM 380, Houston, TX 77030. Phone: 713-798-5485; Fax: 713-798-1067; kc1@bcm.edu.
P.L. Ho and E.J. Lay contributed equally to the work.

Note: Supplementary data for this article are available at Cancer Research Online (http://cancerres.aacrjournals.org/).

Authors' Contributions
Conception and design: K.S. Chan
Development of methodology: P.L. Ho, E.J. Lay, K.S. Chan
Acquisition of data (provided animals, acquired and managed patients, provided facilities, etc.): P.L. Ho, E.J. Lay, W. Jian, D. Parra, K.S. Chan
Analysis and interpretation of data (e.g., statistical analysis, biostatistics, computational analysis): P.L. Ho, E.J. Lay, K.S. Chan
Writing, review, and/or revision of the manuscript: P.L. Ho, E.J. Lay, K.S. Chan
Administrative, technical, or material support (i.e., reporting or organizing data, constructing databases): P.L. Ho, E.J. Lay, K.S. Chan
Study supervision: K.S. Chan

Disclosure of Potential Conflicts of Interest
No potential conflicts of interest were disclosed.

Introduction

Bladder cancer is the fifth most common cancer with 69,250 new cases annually in the United States. Urothelial carcinoma represents approximately 90% of bladder cancers, which arise from an epithelial origin. Two subtypes of bladder urothelial carcinomas exist: noninvasive papillary and muscle-invasive cancer. Evidence supports that these 2 subtypes develop through their own independent pathologic and molecular pathways, although certain overlap does exist (1-4). The vast majority of muscle-invasive cancers arise *de novo* from carcinoma *in situ* (CIS) without prior clinical progression through noninvasive papillary lesions (2, 4). Muscle-invasive bladder cancer is clinically unfavorable with only a 5-year overall survival of 48% to 67% even after radical cystectomy (removal of entire bladder) for localized disease (5).

Several signaling pathways, such as p53, pRB, PTEN, and their downstream interacting proteins, have been described in mediating the development of invasive bladder cancer (6-9). For instance, *TP53* mutation and RB inactivation are common in human bladder CIS (7, 8) and invasive cancer (6) and were shown to be associated with poor prognosis (10, 11). However, mouse model carrying urothelial specific deletions of *p53* and *pRB* only produced late-onset hyperplasia and low-grade noninvasive papillary bladder tumors (12). Exposure of these urothelial specific p53/pRB-deficient mice to subcarcinogenic dose of the carcinogen, *N*-butyl-*N*-(4-Hydroxybutyl) nitrosamine (BBN), led to 50% incidence of invasive bladder cancer, whereas single knock out mice of p53 or pRB did not develop invasive cancer in response to BBN (12). Independently, lack of PTEN protein in human bladder cancer is shown to associate with poor outcome, and mouse urothelial specific deletions of PTEN and p53 via an adeno-Cre delivery system to the bladder induces invasive cancer development (9). Despite the current understanding of signaling pathways and mouse models for invasive bladder cancer, a mouse model representing the unique clinical progression of invasive bladder cancer directly from CIS, without prior pathologic appearance as noninvasive papillary tumor, is lacking. In this study, we describe a novel mouse model that targets an active dimerized form of Stat3 to the basal cells of bladder epithelium (urothelium). When Stat3 is constitutively active, the carcinogen BBN induced rapid progression of urothelial progenitor cells to CIS formation and subsequent muscle-invasive cancer. This mouse model implicates a role for Stat3 in predisposing urothelial basal cells toward *de novo* CIS formation and invasive cancer development, which closely resembles the clinical pathogenesis of human invasive bladder cancer.

Materials and Methods

K5.Stat3-transgenic mice and nitrosamine (BBN) treatment protocol

K5.Stat3-transgenic mice were characterized as previously described (13). Adult transgenic mice and wild-type litter-mates at 6 to 8 weeks of age were treated with 0.05% BBN in drinking water for 12 weeks, followed by regular drinking water. Mice were sacrificed at 1 week ($n = 4$), 2 weeks ($n = 4$), 4 weeks ($n = 4$), 6 weeks ($n = 4$), 13 weeks ($n = 4$), and 20 weeks ($n = 42$) after first BBN treatment. Mouse bladders were either fixed in 10% formalin and paraffin embedded for histologic analyses or freshly dissociated for *in vitro* tumor-sphere forming assay.

Immunostaining and Western blotting

Tumor sections were analyzed following standard hematoxylin and eosin (H&E) procedures or immunohistochemical analysis protocols (Dako; ref. 14). Nikon microscopy system and NIS Elements software were used for imaging and semiautomated quantification of $CK14^+$ and $CK18^+$ cells. Primary antibodies used are listed as follows: Flag (Sigma F1804), Stat3

(Cell Signaling 9139), pTyrStat3 (Cell Signaling 4113), CK14 (Convance PRB-155P), CK5 (Abcam ab75869), CK18 (Abcam ab668), and cleaved caspase-3 (Cell Signaling 9661).

Tumor-sphere forming assay

Bladder tumors were enzymatically dissociated into single-cell suspension as previously described (14), and their ability to generate sphere-forming stem cell colonies was analyzed in an *in vitro* assay as previously described (15). In brief, viable single-cell suspension of tumor cells were resuspended in 1:1 ratio of serum-free Keratinocyte Growth Media (Gibco/Invitrogen) and Growth Factor Reduced Matrigel (BD Biosciences, 356231). Tumor sphere formation was assayed 12 days after first plated.

Animal care and patient materials

All animal procedures were approved under protocol AN-5529, and all patient materials were approved under Institutional Review Board protocol H-26809.

Results and Discussion

Urothelial characterization of Stat3-transgenic mice

Stat3 is a latent transcription factor that normally resides in the cytoplasm. Upon growth factor/cytokine receptor or non-receptor tyrosine kinase-mediated activation, Stat3 rapidly translocates into the nucleus where it binds to consensus promoter region and activates target gene transcription (16). The association of Stat3 to human invasive bladder cancer and poor survival has been reported (14, 17). However, its biologic role in *de novo* bladder tumorigenesis has not been fully explored. We previously reported the generation of transgenic mice overexpressing a dimerized form of active Stat3 (Stat3C; ref. 18) by targeting its expression to epithelial basal cells via the keratin 5 promoter (ref. 13; Supplementary Fig. S1A). Here, we investigated the relevance of these transgenic mice in modeling the pathogenesis of human-invasive bladder cancer by exposing them to a well-established chemical carcinogen regimen BBN for inducing rodent bladder cancer (19). Transgene expression in the mouse bladder of Stat3-transgenic mice was first validated by Western blot analysis of Flag protein expression, a polypeptide that was tagged onto the Stat3 transgene (Supplementary Fig. S1B). The urothelial over-expression of Stat3 protein was 5.6-fold greater in Stat3-transgenic mice compared with wild-type littermates, as shown by densitometry analysis (Supplementary Fig. S1B). The restricted expression of Stat3 to the nucleus of urothelial basal cells was determined by immunohistochemistry (Supplementary Fig. S1C and D).

N-butyl-N-(4-hydroxybutyl)nitrosamine induces immediate progression into carcinoma *in situ* in Stat3-transgenic mice

Although hyperplasia was evident in bladder urothelium of Stat3-transgenic mice, spontaneous bladder tumors were not observed after 14 to 16 months of age [Fig. 1A (TG, $n = 14$) and Fig. 1G (WT, $n = 9$)], suggesting active Stat3 signaling alone is not sufficient for driving bladder tumorigenesis. After short exposure to the carcinogen BBN, dysplastic lesions resembling CIS were evident in Stat3-transgenic mice as early as 1 week after carcinogen treatment (Fig. 1B). Early invasion into the lamina propria was observed at 2 weeks (Fig. 1C), and invasive cancer was evident at 4 weeks (Fig. 1D) after first carcinogen treatment. These CIS lesions are characterized by atypical cellular morphology from basal, intermediate, to umbrella cells, and almost the entire urothelium analyzed contained CIS in Stat3-transgenic mice (Fig. 1A–D). Careful analyses of these early lesions did not reveal evidence of noninvasive tumors. These results implicated a role for Stat3 in predisposing carcinogen-initiated urothelial cells to rapid progression into CIS, which bypassed noninvasive tumor stage. In contrast, in BBN-treated wild-type mice, both urothelial

hyperplasia and focal CIS were observed as premalignant lesions in the bladder (Fig. 1H–J). These results suggested that in wild-type mice, carcinogen-induced bladder tumorigenesis could go through both pathologic pathways: (i) step-wise progression from urothelial hyperplasia into nonmuscle invasive papillary tumors and eventually muscle-invasive bladder cancer, or (ii) CIS into muscle-invasive bladder cancer. However, due to the limitation of the current model, it is impossible to trace the fate of these early lesions from wild-type mice and specifically pinpoint the pathologic pathway followed during tumor progression.

N-butyl-N-(4-hydroxybutyl)nitrosamine induces invasive bladder cancer in Stat3-transgenic mice

At 20 weeks after first BBN treatment, 100% of Stat3-transgenic mice developed grossly visible muscle-invasive bladder cancers (Supplementary Fig. S1E), which were confirmed by H&E staining in histologic sections showing microscopic invasion into muscle bundles (Fig. 1E and F). On the other hand, development of either hyperplasia or noninvasive cancer was seen in 41.38% of age-matched wild-type mice (Fig. 1K), whereas 58.62% developed invasive bladder cancer (Fig. 1L). Kaplan–Meier analysis revealed a better survival of wild-type mice than survival of Stat3-transgenic mice (Supplementary Fig. 1F). The expression of Stat3 has a reported association with invasive properties and poor clinical prognosis in human bladder cancer (14, 17). The distinct bladder tumor phenotype from Stat3-transgenic mice versus wild-type littermates in this carcinogenesis experiment clearly supports an involvement of active Stat3 in *de novo* development of early CIS and muscle-invasive cancer. Another phenotype worth highlighting in Stat3-transgenic mice is the rapid progression into CIS and invasive cancer, without prior appearance as noninvasive tumors. In human bladder cancer, 70% to 80% go through a stepwise progression from hyperplasia to noninvasive papillary tumor, but a majority of these tumors do not progress into invasive cancer (Supplementary Fig. S2A, D, and E). The cancer progression in Stat3-transgenic mice closely resembles the alternative pathway in humans from CIS to invasive bladder cancer (Supplementary Fig. S2A–C). However, it should be noted that Stat3 is unlikely the only pathway that can drive the development of BBN-induced invasive bladder cancer, as only approximately 30% of invasive bladder cancer from wild-type mice showed nuclear localization of Stat3 (data not shown).

BBN-induced premalignant lesions in Stat3-transgenic mice showed an early expansion of $CK14^+$ stem cells

We have previously reported bladder cancer patients with a higher frequency of $CK14^+$ cancer stem cells associate with poor survival outcome in 2 independent patient cohorts (20). Because bladder cancer with poor survival outcome are primarily high-grade invasive cancer, we hypothesized that active Stat3 may regulate a possible expansion of $CK14^+$ stem cell in this transgenic mouse model, which subsequently leads to early CIS and invasive cancer progression. To test our hypothesis, we set off to examine the relative expression of stem and differentiated cell markers in bladder tumors derived from Stat3-transgenic mice in comparison with that from wild-type littermates. We recently reported CK14 as a primitive stem cell marker precursor to CK5 in human bladder cancer (20). CK14 is an acidic type I cytokeratin that commonly heterodimerizes with the basic type II cytokeratin CK5, and it is perceived that they coexpress within the same urothelial cells. Immunohistochemical staining of urothelium from young adult wild-type mouse revealed that CK5 is expressed continuously throughout the basal cell layer (Fig. 2F). Interestingly, CK14 expressing cells is scattered and represents only a subpopulation of $CK5^+$ urothelial cells (Fig. 2E, marked by arrows). These staining patterns agree with the concept that $CK14^+$ cells are a sub-population and may be precursor to $CK5^+$ urothelial cells, although lineage-tracing is required for definitive proof. We therefore proceeded to use CK14 as a putative stem/

progenitor cell marker and CK18 as a more differentiated cell marker to compare the relative frequency of these cellular compartments in premalignant lesions or bladder tumors derived from Stat3-transgenic mice and wild-type littermates. Premalignant CIS lesions induced by BBN in Stat3-transgenic mice showed a significant expansion of $CK14^+$ cells into at least 3 to 6 cell layers (Fig. 2C and J) as compared with early hyperplastic lesions induced by BBN in wild-type mice, which had a smaller expansion of $CK14^+$ cells to form a continuous layer in urothelial basal cells ($P < 0.0001$) and a greater single layer of $CK18^+$ differentiated superficial cells (Fig. 2G and J, $P = 0.0002$). In noninvasive papillary tumor induced by BBN in wild-type littermates, a significant proportion of tumor cells retain a distribution of more differentiated tumor cells marked by CK18 (Fig. 2H, red), although a clonal outgrowth of $CK14^+$ cells (20.6%) was also observed (Fig. 2H, green color). In invasive bladder tumors induced by BBN in wild-type mice, there is an increase of $CK14^+$ tumor cells to 61.3% with the presence of $CK18^+$ differentiated cells (Fig. 2I, higher magnification in Supplementary Fig. S3A–D), whereas in invasive bladder tumors induced by BBN in Stat3-transgenic mice, $CK18^+$ differentiated cells are completely absent (0%) with predominantly $CK14^+$ stem cells (77.0%, Fig. 2D, higher magnification in Supplementary Fig. S3E–H). Statistical analysis revealed a significant difference in the percentage of $CK14^+$ stem cells in invasive cancer derived from Stat3-transgenic mice, in comparison with both noninvasive and invasive tumors derived from wild-type littermates (Fig. 2K, $P < 0.0001$ and $P = 0.01$, respectively). These results revealed that a shift of balance toward $CK14^+$ stem cells is evident in invasive bladder tumors from both Stat3-transgenic mice and wild-type mice, although more significant in that from Stat3-transgenic mice. Therefore, Stat3 is unlikely the only pathway that can drive expansion of $CK14^+$ stem cells in invasive bladder tumors. Nevertheless, active Stat3 clearly contributed to a significant expansion of $CK14^+$ stem cells in early CIS that likely contributed to subsequent invasive tumor formation in Stat3-transgenic mice.

Stat3-driven bladder tumors contain a higher frequency of sphere-forming stem cells

To examine the validity of $CK14^+$ tumor cells as functional stem cells, we have successfully adapted an *in vitro* assay to analyze the frequencies of sphere-forming stem cells in corresponding bladder tumors derived from BBN-treated Stat3-transgenic mice and those from wild-type littermates (15, 21). Interestingly, when equal numbers of tumor cells were analyzed in this assay, Stat3-driven bladder tumor cells generated a significantly higher number of sphere-forming stem cells in comparison with wild-type littermates (Fig. 3A, $P = 0.02$). These results are consistent with earlier immunofluorescence staining, confirming the increase of $CK14^+$ cells in BBN-induced bladder tumors in Stat3-transgenic mice (Fig. 2D and K) are indeed functional stem cells. Although the sphere size difference was not statistically significant (Fig. 3B), a small proportion of tumor cells from BBN-induced Stat3-transgenic mice generated spheres that are larger in size (>90 μm; Fig. 3B and D) than the regular size (35–90 μm) generated from BBN-induced wild-type tumors (Fig. 3E). We attempted to serially passage these spheres *in vitro*. Unfortunately, these primary tumor spheres seemed to secrete extracellular matrix that made it technically challenging to enzymatically retrieve viable cells for serial passaging (data not shown). As a complementary approach, we overexpressed Stat3C in mouse bladder carcinoma cell line MB49, and Stat3C MB49 cells showed higher sphere formation in primary and secondary passages compared with control (Supplementary Fig. S4A and B).

Active Stat3 confers urothelial cell survival in response to carcinogen treatment

Next, we explored the potential mechanisms leading to this significant expansion of $CK14^+$ stem cells in lesions from BBN-treated Stat3-transgenic mice, in comparison with that from BBN-treated wild-type littermates. Because Stat3 has a recognized antiapoptotic role by mediating downstream expression of Bcl-XL, we hypothesized that Stat3 may confer better

survival of urothelial cells in response to carcinogen treatment. In early lesions treated by BBN, we examined the frequency of caspase-3–positive cells to quantify apoptotic cells. In wild-type and Stat3-transgenic premalignant lesions, we observed a portion of caspase-3–positive cells within the $CK14^-$ superficial layers (Fig. 3F and G, marked by arrows), as well as some caspase-3–positive cells within $CK14^+$ cell layers (Fig. 3F–I, marked by asterisk). There was not a significant difference in apoptotic cells within the $CK14^+$ cells of wild-type and Stat3-transgenic mice (Fig. 3J). Interestingly, within the $CK14^-$ cells, there was an unexpected increase in the percentage of apoptotic cells in the early lesions from Stat3-transgenic mice in comparison with that from wild-type littermates (Fig. 3J, $P = 0.007$). We reasoned that although Stat3 protects $CK14^+$ cells from BBN-induced apoptosis, it is not targeted to $CK14^-$ superficial cells (Supplementary Fig. S1D). Therefore, BBN might preferentially induce apoptosis of $CK14^-$ cells in Stat3-transgenic mice. This might provide a possible mechanistic insight into the significant expansion of $CK14^+$ cell compartment in early lesions from Stat3-transgenic mice, in comparison with wild-type control. In wild-type tumors, there was an overall and statistically significant increase in apoptotic index in invasive versus noninvasive tumors (Fig. 3K, $P = 0.002$), which is consistent with a previous report on BBN-induced rodent bladder tumors (22). Interestingly, invasive tumors from Stat3-transgenic mice exhibit a significant reduction in apoptotic index, in comparison with invasive tumors from wild-type littermates (Fig. 3K, $P = 0.004$). Antiapoptotic role of Stat3 at this later stage of tumorigenesis may be important for survival of cancer cells that have accumulated additional alterations for malignant progression.

Association of nuclear Stat3 localization with $CK14^+$ tumor cells in human bladder cancer patient

To examine the human relevance of these bladder tumor results from mice, which implicate a role of Stat3 in invasive progression, we analyzed 8 early-stage (6 pTa LG, 2 Ta HG) and 8 advanced stage human bladder cancers (1 TIS, 2 pT2, 5 pT3; Supplementary Table S1). In early-stage bladder tumors, we observed that 37.5% (3 of 8) express nuclear active Stat3, whereas 100% (8 of 8) of higher stage bladder cancers expressed nuclear active Stat3 (Supplementary Table S1). Immunohistochemical analysis of representative sections from higher stage tumors with nuclear expression of active Stat3 (Fig. 4A and C) revealed that they also predominantly express $CK14^+$ stem cells (Fig. 4B and D). In contrast, representative sections from pTa low-grade tumors revealed a lack of nuclear Stat3 staining (Fig. 4E and G) and CK14 staining (Fig. 4F and H).

Collectively, these results from Stat3-transgenic mice and human bladder cancer for the first time implicate a role for Stat3 in predisposing urothelial basal cells toward the CIS progression pathway into invasive bladder cancer. Because chronic inflammation induced by cigarette smoking and persistent urinary tract infections have been shown to be a promoting factor for bladder cancer (23), Stat3 activation may be an important downstream mediator to inflammatory cytokines such as interleukins (IL-17 and IL-6) during bladder tumorigenesis. Further studies to identify the upstream activators for Stat3 and to investigate its expression in a large human cohort of human CIS and invasive bladder cancer will likely reveal its significance in driving urothelial cells toward the pathway of CIS and invasive cancer progression. This unique mouse model reported in this study will provide a valuable platform to understand other interacting pathways in driving CIS and invasive bladder cancer progression.

Supplementary Material

Refer to Web version on PubMed Central for supplementary material.

Acknowledgments

The authors thank Dr. John DiGiovanni and Steve Carbajal in coordinating the transfer of Stat3-transgenic mice used for research in this study, Dr. Li Xin for his expertise and advice in the sphere-forming assay, Dr. Jonathan Levitt for providing MB49 cells, Antonina Kurtova for her technical assistance, Dr. Michael Ittmann, Dr. Sayeeduddin Mohammad, and Dan L. Duncan Cancer Center Human Tissue and Pathology (HTAP) Core Resource for their consultation and services, and Dr. Carolyn Smith and Dr. David Rowley for their editorial comments.

Grant Support

This work was supported by grant funding from NCI R00 CA129640-05 (to K.S. Chan), V Foundation for Cancer Research V Scholar Award (to K.S. Chan), and gift fund from Bladder Cancer Partnership (to K.S. Chan).

References

1. Dinney CP, McConkey DJ, Millikan RE, Wu X, Bar-Eli M, Adam L, et al. Focus on bladder cancer. Cancer Cell. 2004; 6:111–6. [PubMed: 15324694]
2. Wu XR. Urothelial tumorigenesis: a tale of divergent pathways. Nat Rev Cancer. 2005; 5:713–25. [PubMed: 16110317]
3. Mitra AP, Datar RH, Cote RJ. Molecular pathways in invasive bladder cancer: new insights into mechanisms, progression, and target identification. J Clin Oncol. 2006; 24:5552–64. [PubMed: 17158541]
4. Goebell PJ, Knowles MA. Bladder cancer or bladder cancers? Genetically distinct malignant conditions of the urothelium. Urol Oncol. 2010; 28:409–28. [PubMed: 20610279]
5. Malkowicz SB, van Poppel H, Mickisch G, Pansadoro V, Thuroff J, Soloway MS, et al. Muscle-invasive urothelial carcinoma of the bladder. Urology. 2007; 69:3–16. [PubMed: 17280906]
6. Cairns P, Proctor AJ, Knowles MA. Loss of heterozygosity at the RB locus is frequent and correlates with muscle invasion in bladder carcinoma. Oncogene. 1991; 6:2305–9. [PubMed: 1766677]
7. Hruban RH, van der Riet P, Erozan YS, Sidransky D. Brief report: molecular biology and the early detection of carcinoma of the bladder–the case of Hubert H. Humphrey. N Engl J Med. 1994; 330:1276–8. [PubMed: 7993407]
8. Hartmann A, Schlake G, Zaak D, Hungerhuber E, Hofstetter A, Hofstaedter F, et al. Occurrence of chromosome 9 and p53 alterations in multifocal dysplasia and carcinoma *in situ* of human urinary bladder. Cancer Res. 2002; 62:809–18. [PubMed: 11830537]
9. Puzio-Kuter AM, Castillo-Martin M, Kinkade CW, Wang X, Shen TH, Matos T, et al. Inactivation of p53 and Pten promotes invasive bladder cancer. Genes Dev. 2009; 23:675–80. [PubMed: 19261747]
10. George B, Datar RH, Wu L, Cai J, Patten N, Beil SJ, et al. p53 gene and protein status: the role of p53 alterations in predicting outcome in patients with bladder cancer. J Clin Oncol. 2007; 25:5352–8. [PubMed: 18048815]
11. Shariat SF, Bolenz C, Karakiewicz PI, Fradet Y, Ashfaq R, Bastian PJ, et al. p53 expression in patients with advanced urothelial cancer of the urinary bladder. BJU Int. 2010; 105:489–95. [PubMed: 19659466]
12. He F, Mo L, Zheng XY, Hu C, Lepor H, Lee EY, et al. Deficiency of pRb family proteins and p53 in invasive urothelial tumorigenesis. Cancer Res. 2009; 69:9413–21. [PubMed: 19951992]
13. Sano S, Chan KS, Carbajal S, Clifford J, Peavey M, Kiguchi K, et al. Stat3 links activated keratinocytes and immunocytes required for development of psoriasis in a novel transgenic mouse model. Nat Med. 2005; 11:43–9. [PubMed: 15592573]
14. Chan KS, Espinosa I, Chao M, Wong D, Ailles L, Diehn M, et al. Identification, molecular characterization, clinical prognosis, and therapeutic targeting of human bladder tumor-initiating cells. Proc Natl Acad Sci U S A. 2009; 106:14016–21. [PubMed: 19666525]
15. Xin L, Lukacs RU, Lawson DA, Cheng D, Witte ON. Self-renewal and multilineage differentiation *in vitro* from murine prostate stem cells. Stem Cells. 2007; 25:2760–9. [PubMed: 17641240]
16. Yu H, Pardoll D, Jove R. STATs in cancer inflammation and immunity: a leading role for STAT3. Nat Rev Cancer. 2009; 9:798–809. [PubMed: 19851315]

17. Mitra AP, Pagliarulo V, Yang D, Waldman FM, Datar RH, Skinner DG, et al. Generation of a concise gene panel for outcome prediction in urinary bladder cancer. J Clin Oncol. 2009; 27:3929–37. [PubMed: 19620494]

18. Bromberg JF, Wrzeszczynska MH, Devgan G, Zhao Y, Pestell RG, Albanese C, et al. Stat3 as an oncogene. Cell. 1999; 98:295–303. [PubMed: 10458605]

19. Bryan GT. The pathogenesis of experimental bladder cancer. Cancer Res. 1977; 37:2813–6. [PubMed: 326392]

20. Volkmer JP, Sahoo D, Chin RK, Ho PL, Tang C, Kurtova AV, et al. Three differentiation states risk-stratify bladder cancer into distinct subtypes. Proc Natl Acad Sci U S A. 2012; 109:2078–83. [PubMed: 22308455]

21. Chan KS, Volkmer JP, Weissman I. Cancer stem cells in bladder cancer: a revisited and evolving concept. Curr Opin Urol. 2010 Sep.:20393–7.

22. Zhang X, Takenaka I. Apoptosis and carcinogenesis: morphologic observations in the rat bladder treated with N-butyl-N-(4-hydroxybutyl)nitrosamine. Int J Urol. 1998; 5:262–7. [PubMed: 9624559]

23. Michaud DS. Chronic inflammation and bladder cancer. Urol Oncol. 2007; 25:260–8. [PubMed: 17483025]

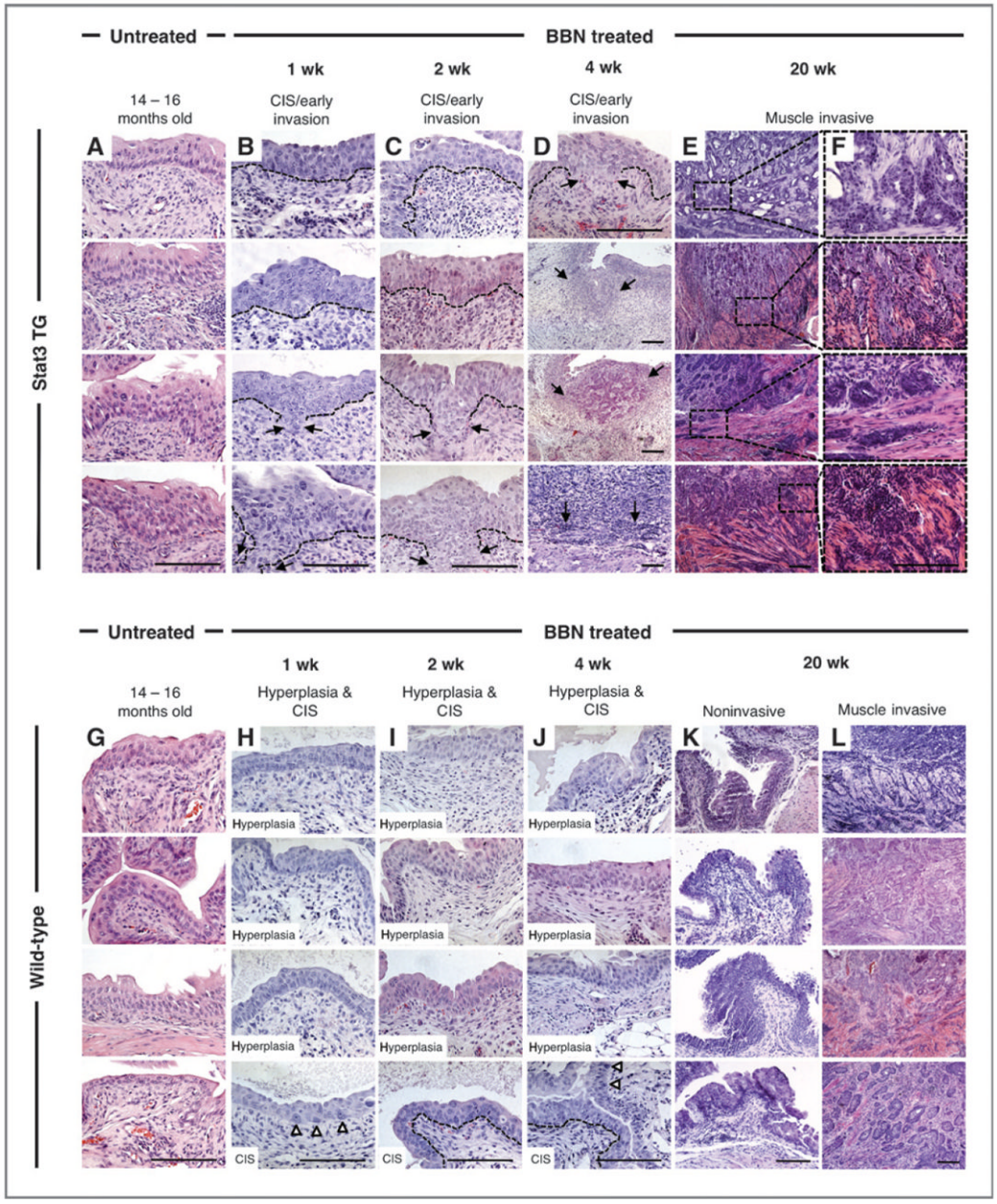

Figure 1.

Stat3 activation predisposes urothelial basal cells to carcinogen-induced CIS and invasive bladder cancer development. H&E staining of bladder urothelium from 4 untreated, aged Stat3-transgenic mice (14 to 16 months old; A); bladder urothelium from 4 Stat3-transgenic mice with CIS and invasion into the lamina propria after 1 week of BBN treatment (B); bladder urothelium from Stat3-transgenic mice with CIS and early invasion into the lamina propria after 2 weeks of BBN treatment (C); CIS and/or invasive bladder cancer after 4 weeks of BBN treatment from Stat3-transgenic mice (D); muscle-invasive cancer in Stat3-transgenic mice 20 weeks after BBN at low magnification (E) and high magnification (F); bladder urothelium from 4 untreated, aged wild-type mice (G); bladder urothelium from wild-type mice with hyperplasia and CIS after 1 week of BBN treatment (H); bladder urothelium from wild-type mice with hyperplasia and CIS after 2 weeks of BBN treatment

(I); bladder urothelium from wild-type mice with hyperplasia and CIS after 4 weeks of BBN treatment (J); noninvasive papillary tumor in wild-type mice 20 weeks after BBN treatment initiation (K); and muscle invasive cancer in wild-type mice 20 weeks after BBN treatment initiation (L). Atypical cells are emphasized with Δ, dotted lines mark the basement membrane, and invasion into the lamina propria or muscle is indicated with black arrows. All scale bars represent 100 μm. TG, transgenic.

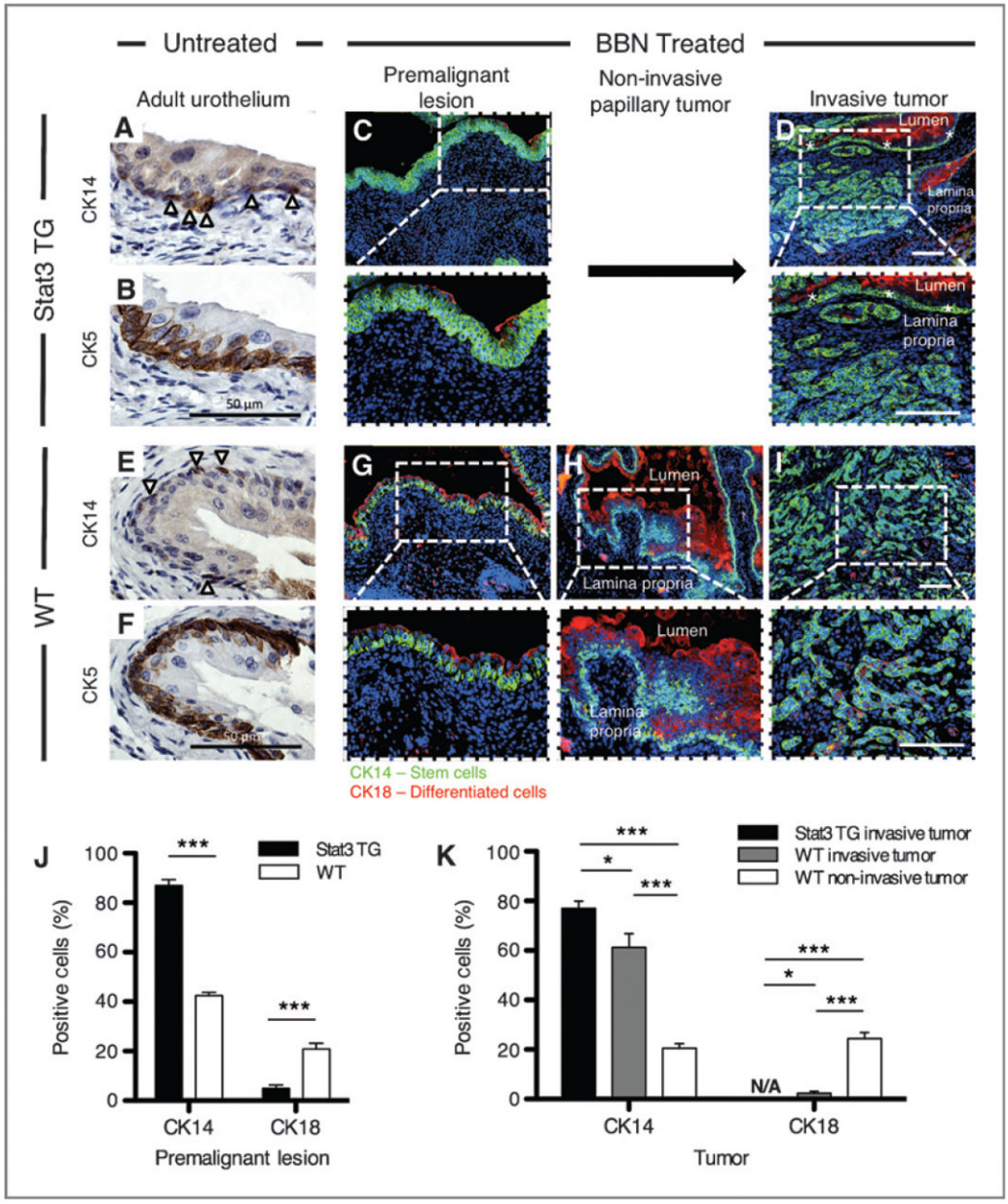

Figure 2.

Stat3 activation leads to expansion of CK14^{+} stem cells in carcinogen-induced bladder lesions. Immunohistochemical analysis of bladder urothelium from untreated adult Stat3-transgenic mice in serial sections with CK14 (marker for stem cells, positive staining indicated with D; A) and CK5 (marker for basal cells; B). Immunofluorescence staining of cytokeratin 14 (CK14, green) and cytokeratin 18 (CK18, red, marker for more differentiated cells) in BBN-induced CIS from Stat3-transgenic mice (low and high magnification; C); and BBN-induced invasive bladder tumor from Stat3-transgenic mice (low and high magnification; D). Immunohistochemical analysis of bladder urothelium from untreated adult wild-type mice with CK14 (E) and CK5 (F). Immunofluoresence staining of CK14 and CK18 in BBN-induced premalignant lesions from wild-type mice (low and high magnification; G); BBN-induced noninvasive papillary bladder tumor from wild-type mice

(low and high magnification; H); and BBN-induced invasive bladder tumor from wild-type mice (low and high magnification; I). J, graph quantifying the percentage of $CK14^+$ and $CK18^+$ epithelial cells in premalignant lesions from Stat3-transgenic and wild-type mice. K, graph quantifying the percentage of $CK14^+$ and $CK18^+$ epithelial tumor cells in Stat3-transgenic invasive tumors, wild-type invasive tumors, and wild-type noninvasive tumors, (***, $P < 0.001$; *, $P < 0.05$). Bladder epithelium is marked with asterisks. Unless otherwise indicated, scale bars represent 100 μm.

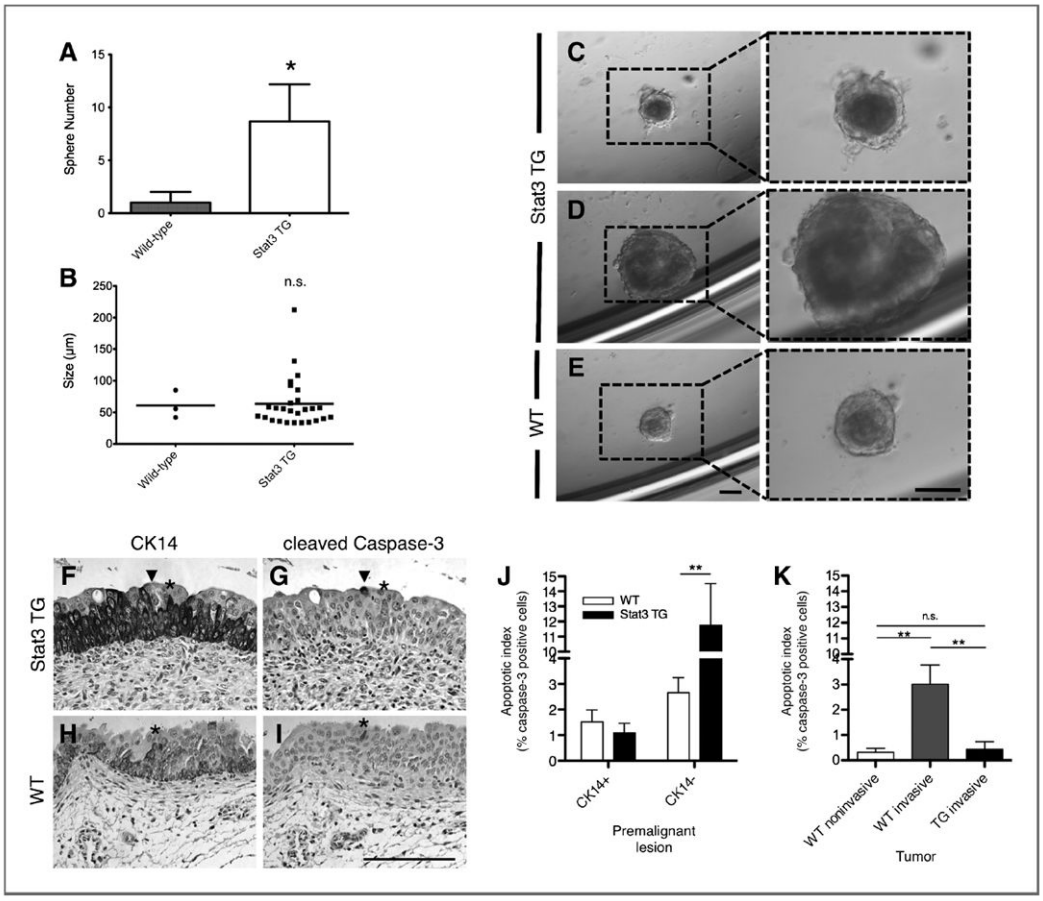

Figure 3.

Stat3 activation in bladder tumors leads to expansion of sphere-forming stem cells. A and B, graph quantifying the number and size of sphere-forming stem cells from BBN-treated wild-type and BBN-treated Stat3-transgenic bladder tumor cells. C, bright field images showing a typical sphere formed from Stat3-transgenic bladder tumor cells (<90μm; low and high magnification). D, bright field images showing a relatively larger size sphere formed from Stat3-transgenic bladder tumor cells (>90μm; low and high magnification). E, bright field images showing a typical sphere formed from wild-type bladder tumor cells (low and high magnification). Immunohistochemical analysis of BBN-induced premalignant lesions from Stat3-transgenic mice in serial sections for CK14 (F) and cleaved caspase-3 (G). Immunohistochemical analysis of BBN-induced premalignant lesions from wild-type mice in serial sections for CK14 (H) and cleaved caspase-3 (I). Asterisks denote active caspase-3 within $CK14^+$ cells, and ▼ denotes cleaved caspase-3 within CK14- cells. J, bar graph quantifying apoptotic index ($CK14^+$ and $CK14^-$ cells) in premalignant lesions from wild-type and Stat3 transgenic. K, bar graph quantifying apoptotic index in wild-type noninvasive papillary tumors, wild-type invasive tumors, and Stat3-transgenic invasive tumors. All scale bars represent 100 μm. **, $P < 0.01$; *, $P < 0.05$; n.s., not significant.

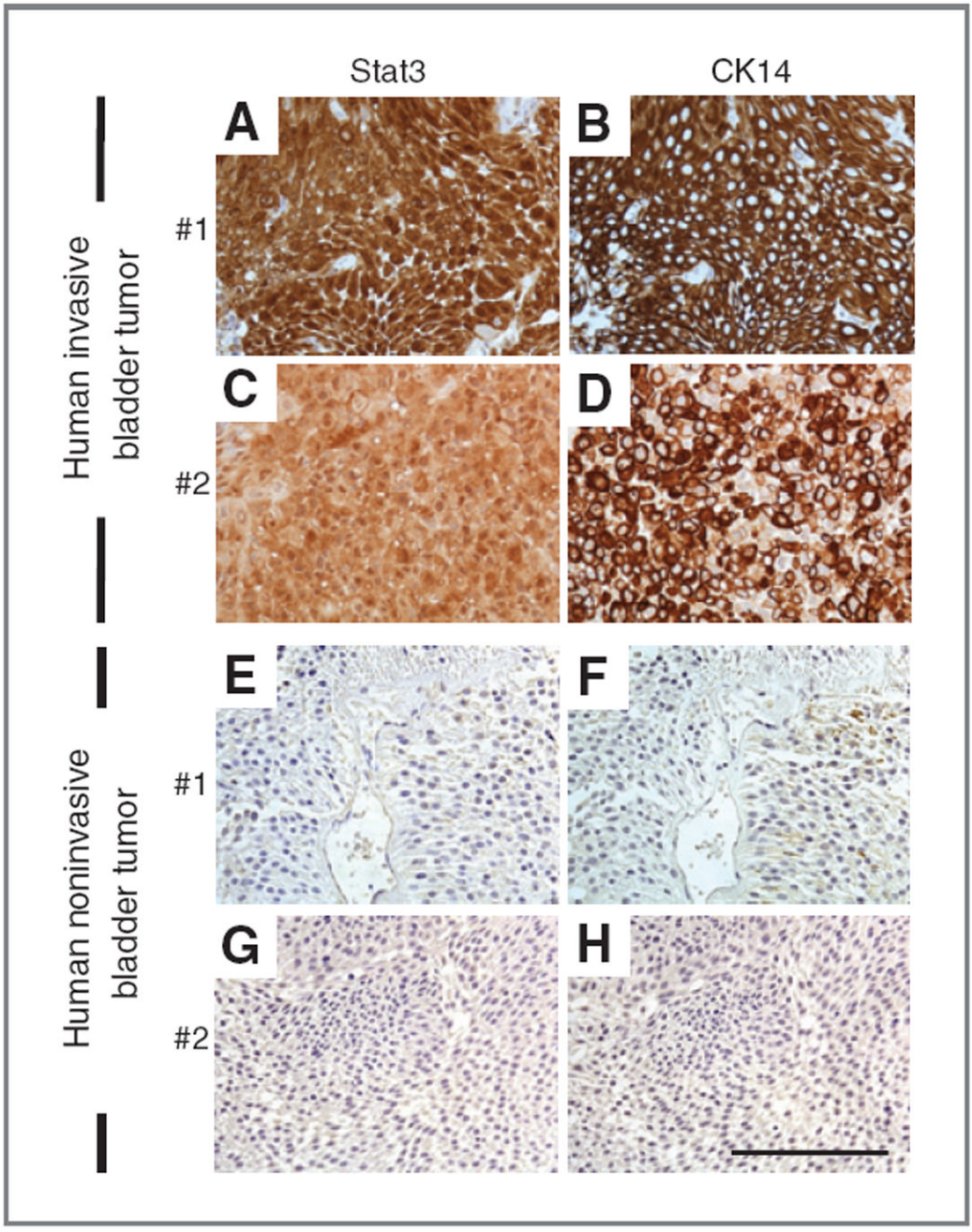

Figure 4.
Nuclear Stat3 and CK14 expression in advanced-stage human bladder cancer. A, C, E, and G, immunohistochemical analysis of nuclear and cytoplasmic Stat3 in human advanced-stage bladder cancer and early-stage noninvasive papillary tumors. B, D, F, and H, immunohistochemical analysis of CK14 in serial sections of human advanced-stage bladder cancer and early-stage noninvasive papillary tumors. Scale bar represents 100 μm.